PHYSICAL REVIEW C **87**, 044308 (2013)

Eight-dimensional calculations of the third barrier in ^{232}Th

P. Jachimowicz
Institute of Physics, University of Zielona Góra, Szafrana 4a, 65516 Zielona Góra, Poland

M. Kowal* and J. Skalski
National Centre for Nuclear Research, Hoża 69, PL-00-681 Warsaw, Poland
(Received 3 January 2013; published 8 April 2013)

We find the height of the third fission barrier B_{III} and energy of the third minimum E_{III} in ^{232}Th using the macroscopic-microscopic model, which is very well tested in this region of nuclei. For the first time it is done on an eight-dimensional deformation hypercube. The dipole distortion is included among the shape variables to ensure that no important shapes are missed. The saddle point is found on a lattice containing more than 50×10^6 points by the immersion water flow method. The shallow third minimum, $B_{\mathrm{III}} - E_{\mathrm{III}} \approx 0.36$ MeV, agrees with the experimental data of Blons *et al.* [Phys. Rev. Lett. **35**, 1749 (1975)]. This is in sharp contrast with the status of the third minima in $^{232-236}$U: their experimental depth of $\geqslant 3$ MeV contradicts all realistic theoretical predictions. We emphasize the importance of repeating the experiment on ^{232}Th, by a technique similar to that used in the uranium nuclei, for settling the puzzle of the third minima in actinides.

DOI: 10.1103/PhysRevC.87.044308 PACS number(s): 25.85.Ca, 21.10.Gv, 21.60.−n, 27.90.+b

I. INTRODUCTION

The search for hyperdeformation (HD), i.e., extremely elongated shapes of atomic nuclei (spheroid with a major to minor axis ratio of 3:1), is one of the most difficult challenges of modern nuclear structure studies. There is still no convincing evidence for discrete γ transitions of HD rotational bands. The only experimental evidence for hyperdeformation, except in light nuclei, has been reported in the region of light actinides, in particular in the uranium isotopes ^{232}U, ^{234}U, and ^{236}U, see [1] and references therein. In these experiments, the fission probability was studied as a function of the excitation energy via different reactions. Strong resonances were observed and a fine structure of some was interpreted as a signature of multiple hyperdeformed bands. Measurements of the angular distribution of the fragments arising from the induced fission support this interpretation. Moreover, by measuring the angular distribution of the fission fragments one can obtain some information about the spin and K quantum number. Due to the predicted static mass asymmetry of the third minima, their intrinsic parity would be broken, so the low-energy excitations should show a pattern of alternating parity (even nuclei) or parity doublet (odd nuclei) bands, different from that in the second minima. Since the third minima are predicted axially symmetric, the excitations would have an approximate (up to a Coriolis mixing, much weaker than in the first or second minimum) K quantum number.

The current experimental status of the third barrier in ^{232}Th is different from that in uranium isotopes. No recent data exist; the only available data are those from 30 years ago [2–5]. In those experiments, conducted by Blons *et al.*, the results pointed to a shallow third minimum (no deeper than 0.5 MeV). Only a little more than 1 MeV deep third minimum in a neighboring nucleus ^{232}Pa was recently reported by the Munich-Debrecen group [6]. The technique used to resolve the observed resonances was the same as in the study of uranium nuclei by the same group. Deep third minima in uranium (3–4 MeV) disagree with all calculations [7–14] except those of S. Ćwiok *et al.*, within the Woods-Saxon model [15–17]. Self-consistent calculations based on the Skyrme SkM* interaction do not give a hyperdeformed minimum in ^{232}Th [7] at all. With the help of a temperature effect, a slight minimum appears, but does not exceed 500 keV. Moreover, with an increasing excitation, the depth of this minimum decreases again. The situation is very similar in ^{232}U and ^{234}U nuclei [8,9]. Self-consistent calculations with the Gogny D1S interaction do not give third minima in those nuclei [11–13] either. Moreover, for ^{236}U, a recent result of Ichikawa *et al.* [14] within the macro-micro approach also does not support the deep minimum reported in [18]: one can read from the map (Fig. 8. in Ref. [14]) that the minimum is not deeper than 300 keV, ten times smaller than the experimental value.

In fact, the hyperdeformed minima predicted in [15–17] were quite abundant: they not only appeared in nuclei where nobody saw them in experiment, but were double, with different octupole deformations $\beta_{30} \approx 0.3$ and 0.6. Contour maps of the potential energy projected on the plane (β_{20}, β_{30}) were calculated via minimization (with the gradient method) over the remaining degrees of freedom. This approach is valid in the case of minima but is rather risky for saddles. As a consequence, one can generate a discontinuous set of shapes [19]. Using the same macro-micro model [this time on the grid with the help of the immersion water flow (IWF) technique] we have showed in [20] that after including the dipole coordinate, both types of the third minima in uranium nuclei disappear completely. The more mass-asymmetric minima were unphysical from the beginning. Their quadrupole moment is large, $Q_{20} \simeq 170$ b, which situates them behind the barrier, closer to the scission point. The existence of minima with a smaller mass asymmetry (and quadrupole moments) requires a more detailed study. Finding the barrier

*m.kowal@fuw.edu.pl

in many-dimensional space requires hypercube calculations. This is the case of ^{232}Th, where the less mass-asymmetric minimum is the deeper one.

Previously, we found in [20] a tentative upper limit of 330 keV for the third barrier in ^{232}Th and 0 in even uranium isotopes $^{232-236}$U by six-dimensional hypercube calculations and by probing various trial eight-dimensional fission paths. The main aim of the present study is to ascertain the prediction for ^{232}Th, showing that a third minimum is there. To accomplish this, an eight-dimensional grid calculation was done. All deformations were treated on the same footing, without introducing any subdivision into relevant and irrelevant subspaces. Let us emphasize that till now only five-dimensional macroscopic-microscopic calculations of fission saddles were available in the literature [14,21,22].

There is one more important motivation for such studies. To distinguish between resonances in the second and third minimum, the excitation energy should be higher than the first barrier but simultaneously lower than the second one. We show that our multidimensional calculations predict such a possibility in ^{232}Th, which is a natural candidate for the future experimental study.

II. METHOD

The energy is calculated within the microscopic-macroscopic method with a deformed Woods-Saxon potential. Nuclear shapes are defined in terms of the nuclear surface [23]. Since we found in [24] that nonaxiality plays an insignificant role at the second barrier,[1] one can expect that in the region of the third barrier, where the shapes become two-fragment-like, triaxiality should be less important than a proper treatment of the axially symmetric shapes. We parametrize the surface as

$$R(\theta) = c(\{\beta\})R_0\left(1 + \sum_{\lambda=1} \beta_{\lambda 0} Y_{\lambda 0}(\theta)\right), \tag{1}$$

where $c(\{\beta\})$ is the volume fixing factor. The macroscopic energy is calculated using the Yukawa plus exponential model [25] with parameters specified in [26]. All other parameters of the model are the same as in a number of our previous studies, e.g., in [24,27,28].

A hyperdeformed minimum was searched by exploring energy surfaces in a region of deformations beyond the second minimum. We generate the grid in axially symmetric deformations:

$$\begin{aligned} &\beta_{10} = -0.35\ (0.05)\ 0.00; && \beta_{20} = 0.55\ (0.05)\ 1.50,\\ &\beta_{30} = 0.00\ (0.05)\ 0.35; && \beta_{40} = -0.10\ (0.05)\ 0.35,\\ &\beta_{50} = -0.20\ (0.05)\ 0.20; && \beta_{60} = -0.15\ (0.05)\ 0.15,\\ &\beta_{70} = -0.20\ (0.05)\ 0.20; && \beta_{80} = -0.15\ (0.05)\ 0.15. \end{aligned} \tag{2}$$

Numbers in the parentheses specify the step with which the calculation is done for a given variable. Thus, we finally have the values of energy at a total of 50 803 200 grid points. On a such giant eight-dimensional grid the IWF saddle-point searching method is used.

III. RESULTS

Let us emphasize that our model, *without* the $\lambda = 1$ term in Eq. (1), very well reproduces first [27] and second [24] barriers and second minima [28] in actinide nuclei. One could hope that an extrapolation to more elongated shapes would be still valid within such a parametrization. What then causes trouble beyond the second peak? It results from the truncation of the expansion (1) that restricts possible shapes for large deformations. Two shapes close to the third saddle are shown in Fig. 1: one from the 8D calculation (β_{10}-β_{80}, in red) and the other from the 7D calculation (β_{20}-β_{80}, in blue). Even if they seem to be not much different, the difference in barrier is 4 MeV. It appears that the dipole deformation β_{10}, usually associated only with a shift of the center of mass, effectively makes up for truncated multipoles in very deformed, mass-asymmetric configurations. We emphasize that our program keeps automatically the center of mass at the coordinate origin: it simply applies an appropriate shift to each shape. Thus β_{10} serves only to probe somewhat different shapes. The deformations that label a given shape are those before the shift (as it was always so in the deformed Woods-Saxon model).

A modification of the energy landscape by including β_{10} is shown in Fig. 2. Since dipole is the first spherical harmonic [Eq. (1)], one can suspect its pronounced effect. Indeed, that effect is significant. Not only is the height of the third saddle clearly reduced, but also the whole landscape is changed. The result indicates a large effect of new shapes, unattainable previously. Figures show also examples of two fission paths. In the version of calculation without the dipole (blue trajectory),

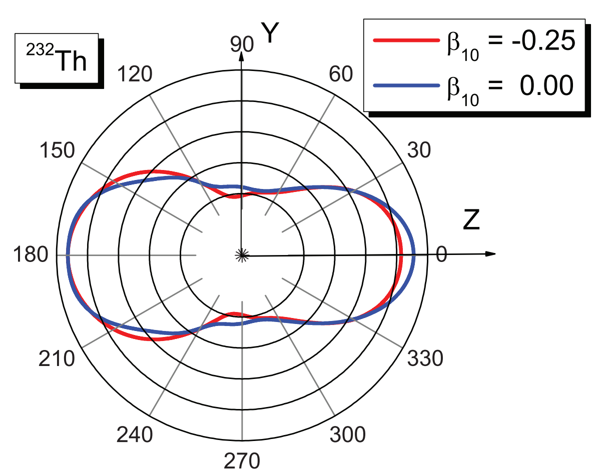

FIG. 1. (Color online) Shapes $R(\theta)/R_0$ (shifted to the center of mass) near the third saddle: red line-8D calculation ($\beta_{10} = -0.25$, $\beta_{20} = 1.25$, $\beta_{30} = 0.00$, $\beta_{40} = 0.10$, $\beta_{50} = 0.10$, $\beta_{60} = -0.05$, $\beta_{70} = -0.05$, $\beta_{80} = 0.00$; $E = 2.2$ MeV); blue line-7D calculation ($\beta_{20} = 1.00$, $\beta_{30} = 0.25$, $\beta_{40} = 0.25$, $\beta_{50} = 0.10$, $\beta_{60} = 0.05$, $\beta_{70} = 0.00$, $\beta_{80} = -0.05$; $E = 6.3$ MeV).

[1] A test was done in a seven-dimensional deformation space including quadrupole nonaxiality but without the dipole variable. For the test we chose ^{248}Cm in which the effect of nonaxiality from the minimization method was the greatest among actinides. Full nine-dimensional calculations with nonaxiality are too time consuming at present.

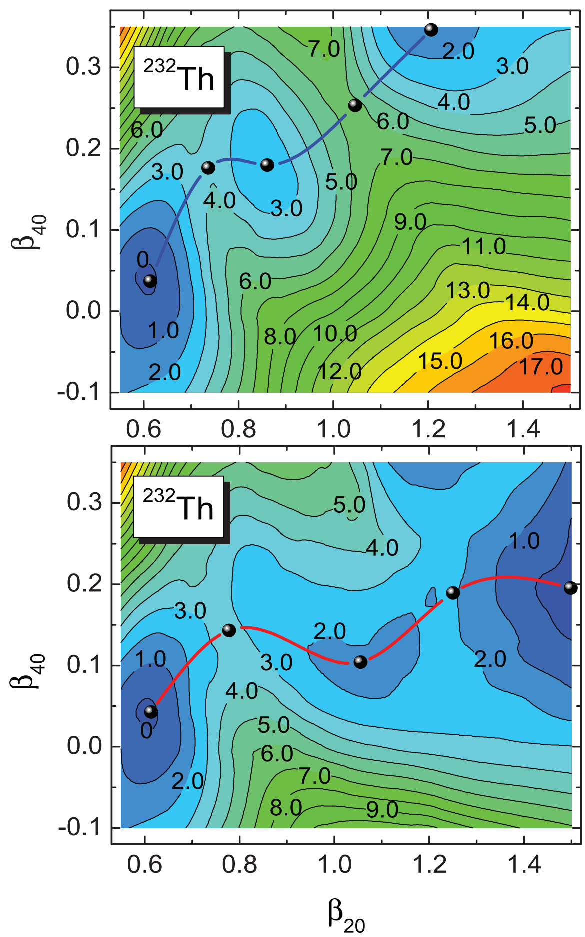

FIG. 2. (Color online) Potential energy surfaces $E(\beta_{20}, \beta_{40})$ for ^{232}Th from the 8D β_{10}-β_{80} calculation; upper panel: at $\beta_{10} = 0$, minimized over the remaining five deformations; bottom panel: minimized over all six remaining deformations, including β_{10}.

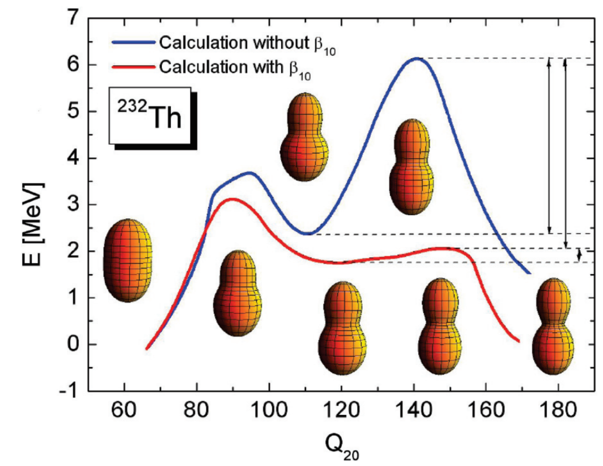

FIG. 3. (Color online) Energy along a sequence of smoothly elongating shapes, beginning at the superdeformed minimum. Corresponding shapes along trajectories are shown.

after passing through the second saddle, the nucleus falls into a deep third minimum. To be split, it needs to tunnel through a more than 4 MeV barrier. When β_{10} is included (red trajectory), after passing the second barrier, the nucleus can easily split. One can notice that β_{10} deformation has almost no effect on the position and height of the second saddle. Precise lowering of the third barrier by β_{10} may be read from Fig. 3 as 4.1 MeV. Besides the significant reduction, one can also see a change in the barrier shape. This rather dramatic change of the fission path in the multidimensional deformation space has a direct effect on fission half-life.

Detailed information about the structure of the fission barrier in ^{232}Th is collected in Table I. The recent theoretical results and experimental data for ^{232}U [30] are also given. It is seen that the model calculation well reproduces essential features of the fission barrier up to superdeformed shapes in both nuclei. The inner fission barrier $B_{\mathrm{I}}^{\mathrm{theor}}$ has been found according to the prescription presented in [27].

Here, a comment is needed. Usually the calculated first saddles are substantially higher than experimental values but the opposite situation takes place in the light thorium isotopes, which is called in the literature the "thorium anomaly". In our case the nonaxiality reduces the first saddle for light thorium only insignificantly, to a nearly proper height (see column 3 of Table I). Thus, the mentioned anomaly does not occur in our case.

To determine the second peak $B_{\mathrm{II}}^{\mathrm{theor}}$, a mass asymmetry is included; details can be found in [24]. One can see that our calculated second minimum and second barrier reasonably agree with experiment. As already mentioned, the experimental situation (when it comes to the depth of hyperdeformed minima) in two isobars ^{232}Th and ^{232}U is completely different. While in ^{232}U, the third minimum is quite deep [30], in ^{232}Th it is very shallow [2–5]. Our results support the existence of a shallow third minimum in ^{232}Th as in the old experiments of Blons and thus agree with the majority of modern theoretical models. Note, that the numbers in Table I for ^{232}Th are not "sensu stricto" experimental values but rather are extrapolated expectation based on the assumption of the triple-humped fission barrier (Fig. 6 in Ref. [32]).

An experiment designed for ^{232}Th, by a technique described in Refs. [1,31], would be crucial for solving the mystery of the third minima in actinides. Particularly promising are experiments employing highly monochromatic γ-ray beams for photofission studies. With a high quality of photon and

TABLE I. Calculated (theor; first row after each isotope) and experimental (expt; rows following the reference numbers) features of the fission barrier in ^{232}Th and ^{232}U. M is the ground state mass excess, B_{I} the first barrier, E_{II} the second minimum, B_{II} the second barrier, E_{III} the third minimum, and B_{III} the third barrier. All quantities (in MeV) are shown relative to the ground state.

Isotope	M^{theor} M^{expt}	$B_{\mathrm{I}}^{\mathrm{theor}}$ $B_{\mathrm{I}}^{\mathrm{expt}}$	$E_{\mathrm{II}}^{\mathrm{theor}}$ $E_{\mathrm{II}}^{\mathrm{expt}}$	$B_{\mathrm{II}}^{\mathrm{theor}}$ $B_{\mathrm{II}}^{\mathrm{expt}}$	$E_{\mathrm{III}}^{\mathrm{theor}}$ $E_{\mathrm{III}}^{\mathrm{expt}}$	$B_{\mathrm{III}}^{\mathrm{theor}}$ $B_{\mathrm{III}}^{\mathrm{expt}}$
^{232}Th	35.33	4.4	2.2	6.1	4.1	4.4
[29]	35.45	5.8		6.7 (6.2)		
[31,32]		5.2 (4.6)	2.4	6.6	2.8	7.0
^{232}U	34.34	4.5	3.2	5.7	0.0	0.0
[29]	34.61	5.4		5.4 (5.3)		
[30]		4.0	3.1	4.9	3.2	6.0

spectral intensity, exceeding the performance of existing facilities by several orders of magnitude seems to be possible in the near future [32]. If the result of Blons *et al.* is confirmed, we will have to understand *why between* ^{232}Th *and* ^{232}U, *two* β *decays away, the energy landscape changes so dramatically*. On the other hand, if in the future experiment, a depth of the third minimum is obtained similar to that in ^{232}U, we will have a total contradiction between theory and experiment. *Assuming that the existing resonances cannot be interpreted otherwise, all current meaningful theoretical models would have to be reconstructed anew to give deep hyperdeformed minima*.

One can expect that in hyperdeformed nuclei, some high particle states at normal deformation become occupied with increasing deformation. Since these are the orbits that are occupied in superheavy nuclei at moderate deformations, the whole question may have some impact on the understanding of superheavy nuclei.

IV. CONCLUSIONS

(i) We have presented for the first time an eight-dimensional hypercube calculation for ^{232}Th. To find the third barrier on a giant grid, the IWF method was applied. After a proper inclusion of the dipole deformation we found the depth of the third minimum of about 0.36 MeV. This would rather exclude spectroscopic studies in the third well.

(ii) Including a dipole distortion lowers the third saddle by more than 4 MeV. It seems likely that with the shape parametrization (1), the dipole deformation is important everywhere when large elongation and necking is combined with a sizable mass asymmetry. For example, it may be the case of the Poincaré shape transition at high spins in medium-heavy nuclei.

(iii) New experimental study dedicated to hyperdeformation in ^{232}Th seems essential for the understanding of the third minima in actinide nuclei.

ACKNOWLEDGMENTS

This work was partially supported by Narodowe Centrum Nauki Grant No. 2011/01/B/ST2/05131. The support of the LEA COPIGAL fund is gratefully acknowledged.

[1] A. Krasznahorkay, in *Handbook of Nuclear Chemistry* (Springer Science + Business Media, New York, 2011), Chap. 5.
[2] J. Blons, C. Mazur, and D. Paya, Phys. Rev. Lett. **35**, 1749 (1975).
[3] J. Blons, C. Mazur, D. Paya, M. Ribrag, and H. Weigmann, Nucl. Phys. A **414**, 1 (1984).
[4] J. Blons, B. Fabbre, C. Mazur, D. Paya, M. Ribrag, and Y. Petin, Nucl. Phys. A **477**, 231 (1988).
[5] J. Blons, Nucl. Phys. A **502**, 121c (1989).
[6] L. Csige *et al.*, Phys. Rev. C **85**, 054306 (2012).
[7] J. D. McDonnell, W. Nazarewicz, and J. A. Sheikh, in Proceedings of the 4th International Workshop on Fission and Fission Product Spectroscopy, 2009 (unpublished).
[8] J. D. McDonnell, Ph.D. thesis, University of Tennesse, 2012.
[9] J. D. McDonnell, W. Nazarewicz, and J. A. Sheikh, arXiv:1302.1165v1.
[10] M. Bender, Ph.D. thesis, Universitat Frankfurt, 1998; M. Bender, P-H. Heenen, and P-G. Reinhard, Rev. Mod. Phys. **75**, 121 (2003).
[11] J. F. Berger, M. Girod, and D. Gogny, Nucl. Phys. A, **502**, 85c (1989).
[12] L. Bonneau, P. Quentin, and D. Samsoen, Eur. Phys. J. A **21**, 391 (2004).
[13] J.-P. Delaroche, M. Girod, H. Goutte, and J. Libert, Nucl. Phys. A **771**, 103 (2006).
[14] T. Ichikawa, A. Iwamoto, P. Möller, and A. J. Sierk, Phys. Rev. C **86**, 024610 (2012).
[15] S. Ćwiok, W. Nazarewicz, J.X. Saladin, W. Płóciennik, and A. Johnson, Phys. Lett. B **322**, 304 (1994).
[16] W. Nazarewicz, S. Ćwiok, J. Dobaczewski, and J. X. Saladin, Acta Phys. Pol. B **26**, 189 (1995).
[17] G. M. Ter-Akopian *et al.*, Phys. Rev. Lett. **77**, 32 (1996).
[18] A. Krasznahorkay *et al.*, Phys. Rev. Lett. **80**, 2073 (1998).
[19] P. Möller and A. Iwamoto, Phys. Rev. C **61**, 047602 (2000).
[20] M. Kowal and J. Skalski, Phys. Rev. C **85**, 061302(R) (2012).
[21] P. Möller, D. G. Madland, A. J. Sierk, and A. Iwamoto, Nature **409**, 485 (2001).
[22] P. Möller, A. J. Sierk, and A. Iwamoto, Phys. Rev. Lett. **92**, 072501 (2004).
[23] S. Ćwiok, J. Dudek, W. Nazarewicz, J. Skalski, and T. Werner, Comput. Phys. Commun. **46**, 379 (1987).
[24] P. Jachimowicz, M. Kowal, and J. Skalski, Phys. Rev. C **85**, 034305 (2012).
[25] H. J. Krappe, J. R. Nix, and A. J. Sierk, Phys. Rev. C **20**, 992 (1979).
[26] I. Muntian, Z. Patyk, and A. Sobiczewski, Acta Phys. Pol. B **32**, 691 (2001).
[27] M. Kowal, P. Jachimowicz, and A. Sobiczewski, Phys. Rev. C **82**, 014303 (2010).
[28] M. Kowal and J. Skalski, Phys. Rev. C **82**, 054303 (2010).
[29] G. N. Smirenkin, IAEA Report INDC(CCP)-359, 1993 (unpublished), http://www-nds.iaea.org/RIPL-3/; A. Mamdouh, J. M. Pearson, M. Rayet, and F. Tondeur, Nucl. Phys. A **644**, 389 (1998), http://www-nds.iaea.org/RIPL-2/.
[30] L. Csige *et al.*, Phys. Rev. C **80**, 011301(R) (2009).
[31] P. G. Thirolf and D. Habs, Prog. Part. Nucl. Phys. **49**, 325 (2002); P. G. Thirolf, D.Dc. thesis, Ludwig-Maximilians-Universitat Munchen, 2003.
[32] P. G. Thirolf *et al.*, EPJ Web Conf. **38**, 08001 (2012).